# CrystEngComm

Accepted Manuscript






ROYAL SOCIETY OF CHEMISTRY

www.rsc.org/crystengcomm

Journal Name

RSCPublishing

COMMUNICATION

# Electrodeposition of Ag nanosheets-assembled microsphere @ Ag dendrites core-shell hierarchical architectures and their application in SERS

Cite this: DOI: 10.1039/x0xx00000x

Received ooth January 2012,
Accepted ooth January 2012

DOI: 10.1039/x0xx00000x

www.rsc.org/

Xiaodan Li[1], Meicheng Li[1, 2,*], Peng Cui[1], Xing Zhao[1], Tiansheng Gu[1], Hang Yu[1], Yongjian Jiang[1] and Dandan Song[1, 2]

[1] State Key Laboratory of Alternate Electrical Power System with Renewable Energy Sources, School of Renewable Energy, North China Electric Power University, Beijing 102206, China

[2] Suzhou Institute, North China Electric Power University, Suzhou 215123, China

**The Ag core-shell hierarchical microstructures, with nanosheets-assembled microsphere as the core and dendrites coated on the surface, have been synthesized by electrodeposition. The growth mechanisms of these Ag microstructures have been systematically investigated through the time-dependent morphological evolution. A transformation stage from microspheres to dendrites was found in the morphological evolution of Ag core-shell hierarchical microstructures, which was affected by deposition time and voltage. Therefore, we obtained various Ag core-shell hierarchical microstructures with adjustable ratio of microsphere core to dendrites shell by controlling deposition voltage. Furthermore, the Ag core-shell hierarchical microstructures exhibit excellent surface-enhanced Raman scattering (SERS) ability, showing great potential as effective SERS substrates.**

The silver micro/nanostructures have drawn much attention to various applications, such as catalysis[1, 2], antibacterial activity[3, 4], sensing[5], solar cell[6] and surface-enhanced Raman scattering (SERS) [7-14], due to their unique physicochemical and photoelectric properties. These properties offered by Ag micro/nanostructures are significantly different according to their shapes and morphologies. Thus, the exploration of novel silver micro/nanostructures and its controllable synthesis with expected structure features are crucial approaches to realize their new applications. Various Ag micro/nanostructures have been studied, including simple particles[15], wires[16], plates[17], dendrites[7, 18] and complex hierarchical structures[8-14]. Among them, hierarchical microstructures stimulate much more attention since they exhibit more advantages (stable, anti-agglomeration, improved SERS performance) than the monomorphological structures[12, 13]. And the Design and fabrication of hierarchical structures by adjusting the structural feature of nanometre-scaled building blocks will promote the tunability of material properties for more special applications.

So far, most of the reported hierarchical Ag microstructures[8-13] are assembled by single structural unit, which limits their properties and applications. By comparison, composite hierarchical Ag microstructures assembled by two or more types of nano-units will be promising to combine the advantages of different nanostructures[6]. Moreover, it is easy to tailor material properties by tuning the nano-unites ratio of composite hierarchical Ag microstructures[14]. These unique superiorities will facilitate the exploitation of the most suitable property for device integration application, such as cells and sensors. In the meantime, further study about the growth mechanism should be promoted to control the synthesis of composite hierarchical Ag microstructures.

Herein, we firstly synthesized an Ag nanosheets-assembled microsphere @ Ag dendrites core-shell hierarchical microstructure via electrochemical deposition. Its structure and morphology can be easily controlled by tuning deposition time and voltage. The reported nanosheets-assembled microspheres[13] and the dendritic structures[18] have been obtained during this process as well. The morphology evolution and formation mechanisms of these microstructures have been investigated in detail. Furthermore, SERS performances of the Ag core-shell hierarchical architecture were conducted to reveal their unique superiority.

Silver nitrate, tartaric acid, boric acid, acetone and ethanol were purchased from National Chemical Agent. All analytical reagents need no further treatment. Fluorine doped tin oxide (FTO) coated glasses were soaked for about 10 min by acetone, and then treated 5 min by ultrasound and deionized water to remove the possible impurities. The electrolyte was composed of the aqueous solution of 4.0 M silver nitrate, 4.0 M tartaric acid and 3.0 M boric acid. Electrochemical deposition was performed with a two-electrode system, where FTO-coated glass was used as the working electrode and graphite plate as a counter electrode. During a typical synthesis process, the electrochemical deposition was carried out at 1.11 V for different deposition time, at room temperature in the same solution. For tuning deposition voltage experiment, the electrochemical deposition was carried out at 0.80V, 1.05 V, 1.26V for 50 min and 1.50V for 30 min in the same solution. After the deposition process, all samples were rinsed 3~5 times with deionized water and dried by high-purity flowing nitrogen.

The distribution, size and morphology of the as-prepared samples were characterized by scanning electron microscopy (SEM) (FEI SIRION 200). The chemical composition and structure of the as-prepared samples were analysed by EDX (FEI SIRION 200) and X-ray diffraction (XRD) (Bruker D8 Advance X-ray diffractometer, Cu-Ka radiation r=0.15406 nm). Transmission electron microscopy (TEM) and High-resolution TEM (HRTEM) measurements were conducted on a Philips-FEI TecnaiG2 F20 S-Twin TEM. For SERS measurement, as-prepared samples rinsed with deionized water were immersed in aqueous Rhodamine 6G (R6G) solutions with concentrations of $10^{-6}$, $10^{-12}$ and $10^{-14}$ for 2 h, and then dried in the atmosphere. To estimate the enhancement factor, 2μL of $10^{-3}$ M and $10^{-11}$ M R6G ethanol solution was dropped on FTO-coated glass and as-prepared samples, respectively. The Raman scattering measurements were carried out on a Raman system (HR800, JY, France) with confocal microscopy. The excitation wavelength was 532nm with a power of 0.1mW. The objective lens used by Raman measurement was ×100 and the spot diameter is 2μm. The acquisition time of Raman signal was 10s.

Figure 1 shows different magnifications of Ag core-shell hierarchical microstructures synthesized by depositing of 50 min at 1.11 V. The low magnification SEM image (Fig. S1a) shows a large number of these structures, demonstrating their good uniformity and dispersion. The higher magnification SEM image (Fig. 1a) gives a complete structure of the Ag core-shell hierarchical microstructure. The partial enlarged detail (Fig. 1b) clearly shows the typical Ag core-shell hierarchical microstructure, which contains an Ag nanosheets-assembled microsphere core and an Ag dendrites shell. The thickness of these nanosheets on microsphere core is about one hundred nanometres and the gaps between them are mostly sub-10 nm (Fig. 1b). The Ag dendrites shell is composed of mass dendrites which have a long main trunk (1μm-5μm) with short side branches (several hundred nanometres or even tens of nanometres). TEM observations (Fig. 2c, d) show a group of nanosheets and an individual dendrite at several magnifications. The results are consistent with the results under SEM investigation. The inset HRTEM image taken from the area labelled in Fig. 2c shows that these nanosheets are well crystallized. And the inset HRTEM image in Fig. 2d shows that the interplanar spacing of the dendrite is 0.24 nm, indicating dominant (111) planet growth. As we know, for Ag crystal, the free energy of the (111) plane is the least one among all the planes, and this structure feature of the core-shell hierarchical microstructures would be beneficial for the performance, which will discuss later in the paper. EDX energy spectrum (Fig. S1b) clearly demonstrates that the composition of Ag core-shell hierarchical microstructure is silver and no other diffraction peaks are observed, indicating its high purity.

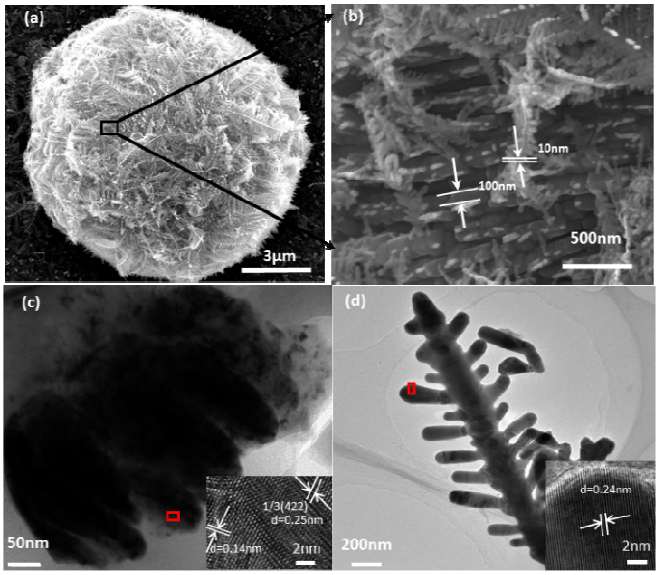


Fig. 1 (a) SEM images of the Ag core-shell hierarchical microstructure. (b) Magnified SEM image of the labelled area on the Ag microstructure as shown in (a). (c) TEM and HRTEM images of the Ag nanosheets; (d) TEM and HRTEM images of the Ag dendrite

In order to obtain a complete insight of the formation process of Ag core-shell hierarchical microstructures, the time-dependent morphological evolution study was conducted. We collected the samples with the deposition time of 10 s (Fig. 2a), 20 s (Fig. 2b), 1 min (Fig. 2c), 5 min (Fig. 2d), 20 min (Fig. 2e) and 50 min (Fig. 2f), respectively. For the samples with very short deposition time (Fig. 2(a, b)), many quasi-spheres can be found on the FTO-coated glass and there are rough particles on the surface of these quasi-spheres. When the deposition time is raised to 1 min (Fig. 2c), the quasi-spheres grow bigger and become more circular than before (Fig. 2b). And the particles on the surfaces become bigger and denser (even merged into smoother sheets). When the deposition time is 5 min (Fig. 2d), the microspheres continue to grow up. Meanwhile, the Ag dendritic nuclei appear both on the surface of microspheres and substrate. These dendrites grow along with the radial direction of the microspheres. And when the deposition time is extended to 20 min (Fig. 2e), the Ag dendrite structures become bigger, longer and denser. After depositing of 50 min, mature Ag core-shell hierarchical microstructures can be obtained (Fig. 2f). Furthermore, as can be seen from the time-dependent morphological evolution study, the size ratio of microsphere core to dendrites shell involved in the Ag core-shell hierarchical microstructure can be regularly controlled by the deposition time.

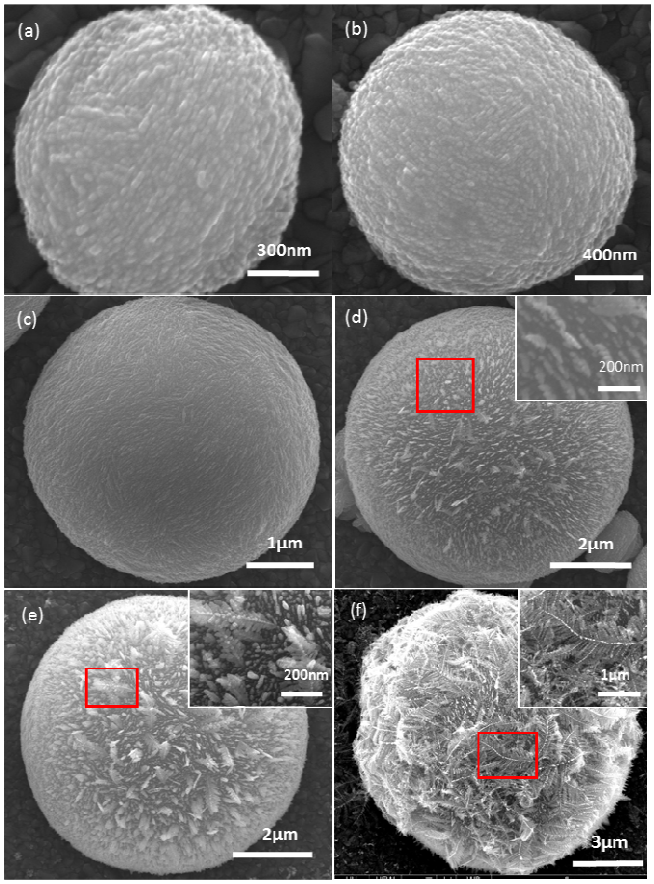


Fig. 2 SEM images of Ag core-shell hierarchical microstructures prepared by electrochemical deposition of different time. (a) 10 s, (b) 20 s, (c) 1 min, (d) 5 min, (e) 20 min, (f) 50min

Based on these results, the growth mechanisms of Ag core-shell hierarchical microstructures are proposed. As can be seen in Fig. 3, at the first stage, the adatoms ($Ag^0$) reduced from $Ag^+$ at the cathodes (FTO) gather to form nanoparticles under the driving force of electric field. Then, aggregations (quasi-spheres) are formed by many self-assembled nanoparticles[13]. At the second stage, the earlier formed quasi-spheres serve as seeds for further aggregation of Ag nanoparticles, evolving into those small microspheres with many rough particles on the surface. As the aggregation progress continues, the adjacent particles begin to form layered nanosheets by Ostwald ripening[19] which makes the surface of microsphere smooth. In the third stage, a transformation stage is formed, during which the new formed nanoparticles begin to assemble in the shape of dendritic structures rather than previous microspheres. During this period, some silver dendrites are too long to stand upright on the surface of microspheres, so they tend to fall down on the microspheres and keep on growing, forming the dendrites shell. Finally, the mature Ag core-shell hierarchical microstructures are formed.

In the whole process, noting that:

(1) There are two reduction reactions in the electrolyte,

$$Ag^+ + e^- \rightarrow Ag$$
$$2H^+ + 2e^- \rightarrow H_2$$

The former is effective reaction and the latter is side reaction for electrochemical deposition.

(2) Two kinds of electrode-potentials are formed in this electrochemical deposition,

$FTO/Ag^+$ (original exist)

$Ag/Ag^+$ (substitution for partial $FTO/Ag^+$ because of deposited Ag on FTO)

(3)Under the FTO/Ag+ electrode-potential, high hydrogen overpotential greatly limits the side reaction; while the $Ag/Ag^+$ electrode-potential can promote the side reaction by decreasing the hydrogen overpotential.[20] In addition, in the replacement reaction, the change of the electrode potential does have effects on the silver nanostructure.[21]

Therefore, at the first stage, the effective discharge and reduction speed are fast and the concentration of new generated adatoms ($Ag^0$) is high. It is known that high reduction speed often causes uneven deposition and particles aggregation, which is unfavourable for anisotropic growth of Ag nanostructures[7]. So, self-assembled Ag particles trend to form spherical aggregations. At the same time, we propose that there is no enough time for most of Ag nanoparticles to merge into the aggregations because of the high $Ag^0$ concentration, which makes the aggregations very rough, as the structure in Fig. 2a.[22] Afterwards, the effect of the $Ag/Ag^+$ electrode potential becomes increasingly significant, resulting that the effective reduction and deposition speed depresses into the range of critical stage. Then assembled Ag nanoparticles begin to show anisotropy, resulting in the formation of dendrites rather than the continued growth of microspheres. In our opinion, this is due to the face-centred cubic structure, that is to say, when the deposition speed becomes low enough, the growth tendency which is more effective along the (111) direction rather than the other directions can dominate assemble process.[18] During the whole growth process, Ostwald ripening plays an important role in the formation of nanosheets and mature dendrites.

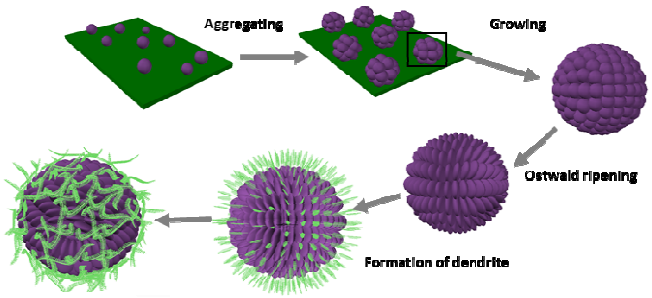


Fig. 3 Schematic illustration of the formation and morphology evolution of Ag core-shell hierarchical microstructures

The transformation stage, as a key point for the transition from microspheres to dendrites, can be regularly controlled not only by changing deposition time but also by tuning deposition voltage. Experimentally, Ag microstructures show different shapes according to different voltages: when the deposition voltage is increased to 1.5 V, the greatly promoted side reaction causes significant reduction of effective deposition speed (less than that of transformation stage). So, the products trend to be (111) planes-dominant silver dendritic structures (Fig. S2a, ESI); conversely, decreasing the deposition voltage to 0.8 V can ensure a fast effective reaction speed. Though the effect of $Ag/Ag^+$ electrode potential continues to be enhanced, the effective deposition speed won't be lower than that of transformation stage yet. Thus, the final products are pure Ag nanosheets-assembled microspheres core (Fig. S2b, ESI). Only when the deposition voltage is in a suitable range (about 1.11V), adding

the effect of $Ag/Ag^+$ electrode potential, the effective reaction can show a qualitative change which means the formation of Ag core-shell hierarchical microstructures. Furthermore, in coincidence with above analysis, the ratio of microspheres core to dendrites shell can be controlled by slightly tuning the deposition voltage at the nearby of 1.11V (Fig S2(c-e), ESI).

To further study the Ag core-shell hierarchical microstructure, we give the XRD spectra of the Ag core-shell hierarchical microstructures, pure nanosheets-assembled microsphere core and pure dendrites (Fig. 4). The four diffraction peaks match well with the (111), (200), (220), and (311) planes of Ag face-centred cubic (fcc) structure (JCPDS, No.04-0783), indicating that they are well crystallized. In addition, the growth of the three Ag microstructures can be analysed by comparing the ratios of (111) to (200) peak intensities. This ratio gives a metric for the relative strength of anisotropic forces in the crystal growth process, where higher ratios are correlated to the preferential stacking of (111) planes.[23] It is clear that dendrites have the highest ratio of (111) to (200) peak intensities, which is consistent with the growth mechanism above.

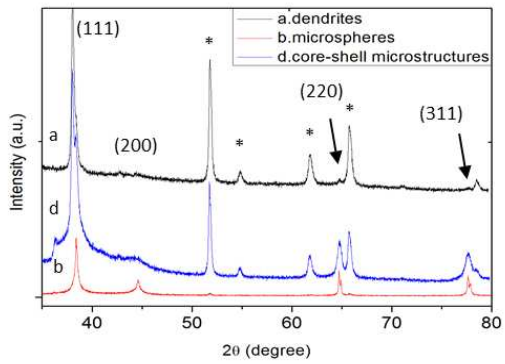


Fig. 4 XRD patterns of (a). dendrites, (b). nanosheets-assembled microspheres, (d). core-shell microstructures shown in Fig. S2, ESI. The asterisk sign (*) indicates the diffraction peaks of FTO.

It is well known that the hot-spots provided by nano/microstructures and the adsorption of probe molecules are two key factors for SERS performance. For example, the (111) planes can adsorb more probe molecules due to their least free energy[24] and the sub-10 nm gaps could provide sufficient hot-spots[12, 13]. In the Ag core-shell hierarchical microstructures, there are nanosheets-assembled microspheres core with sufficient sub-10nm gaps and (111) planet-dominated dendrites shell. We investigated the SERS performances of the core-shell microstructures with different ratio of microspheres core to dendrites shell. Fig 5a depicts the Raman spectra of R6G molecules adsorbed on core-shell microstructures SI, SII, and SIII. The SERS signal intensity of SI for the bands at 612 $cm^{-1}$ is about 1.3 times stronger than that of SII and 3.6 times stronger than that of SIII. This can be explained by the fact that the difference of SERS performance can be attributed to the relationship of adsorption and hot-spots balanced by core-shell structure. SIII is composited of a small sphere core and a thick (111) planet-dominate dendrites shell which can promote the adsorption of probes molecule but invalidate the effect of hot-spots on sphere core. However, SI and SII both have a bigger sphere core with sufficient hot-spots and a thinner (111)-dominate dendrites shell which contributes to adsorb more probe molecules.

To study the SERS sensitivity of Ag core-shell hierarchical microstructures, the SERS spectra of R6G solutions at different concentrations were conducted (Fig. 5b). Many bands of R6G still can be observed in the spectra even when the concentration was down to $10^{-14}$ M, revealing the high sensitivity of Ag core-shell hierarchical microstructure for SERS application. The SERS enhanced factor value of this structure is estimated to be $1.6\times10^8$ for R6G (the method is shown in S3, ESI). As SERS substrate, these samples can be reused after removing the organics adsorbed on its surface by plasma cleaning, because they strongly attach on the substrates. Their retention of high sensitivity for SERS application were demonstrated by the Raman spectra of R6G ($10^{-12}$ M) adsorbed on the sample treated by plasma cleaning (Fig.S4, ESI). These SERS spectra are collected from three individual core-shell hierarchical microstructures, indicating their good reproducibility in the SERS measurement as well.

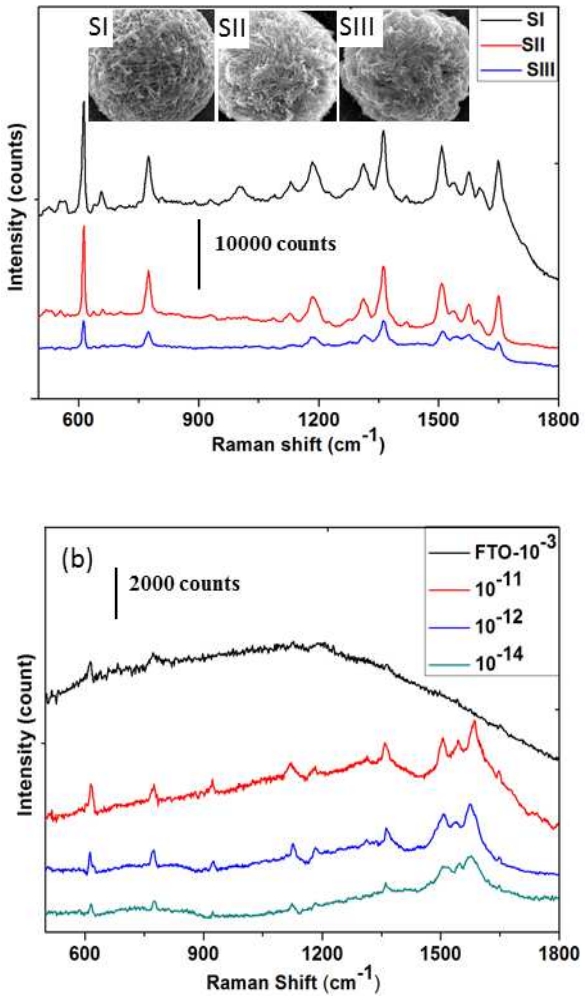


Fig. 5 (a) The SERS spectra of R6G ($10^{-6}$ M) adsorbed on the Ag core-shell microstructures deposited at SI 1.05V, SII 1.11V, SIII 1.26V, corresponding to the structures in Fig. S2(e, d, c), ESI, respectively. (b) The SERS spectra of R6G solutions at different concentrations ($10^{-11}$, $10^{-12}$, $10^{-14}$ M) on as-prepared samples and R6G solution ($10^{-3}$ M) on FTO substrate.

## Conclusions

In summary, Ag nanosheets-assembled microsphere @ Ag dendrites core-shell hierarchical microstructure has been synthesized on FTO substrate via electrochemical deposition. The growth mechanism including transformation stage of this structure has been proposed through time-dependent morphological evolution studies. The structural diversity of this microstructure can be easily realized by tuning deposition time and voltage, which could expand the device application of this material. Furthermore, Ag core-shell hierarchical microstructures show excellent performance in SERS application.

## Notes and references

*This work was supported partially by the National Natural Science Foundation of China (91333122, 51372082, 51172069, 61204064 and 51202067), and Ph.D. Programs Foundation of Ministry of Education of China (20130036110012, 20110036110006), and the Fundamental Research Funds for the Central Universities (Key project 11ZG02).*

† Experimental data on size distribution, morphology, and EDX chemical composition of the microstructures prepared in different conditions were shown in Supplementary Information.

More details about Estimation of enhancement factor were shown in Supplementary Information.

Raman spectra of R6G ($10^{-12}$ M) adsorbed on the samples treated by plasma cleaning were shown in Supplementary Information

Electronic Supplementary Information (ESI) available: [details of any supplementary information available should be included here]. See DOI: 10.1039/c000000x/

1 J. F. Huang, S. Vongehr, S. C.Tang, H. M. Lu, J. C. Shen, X. K. Meng, Langmuir 2009, 25 (19), 11890-11896.
2. J. You, M. X. Xiang, H. Z. Hu, J. Cai, J. P. Zhou and Y. P. Zhang, RSC Advances 2013, 3, 19319-19329
3. S. Pal, Y. K. Tak and J. M. Song, Applied and Environmental Microbiology 2007, 73 (6), 1712-1720
4. V. K. Sharma, R. A. Yngard, Y. Lin, Advances in Colloid and Interface Science 2009, 145, 83-96
5. K. M. Mayer, J. H. Hafner, Chem. Rev. 2011, 111, 3828.
6. X.Chen, B.H.Jia, J.K.Saha, B.Y.Cai, N.Stokes, Q.Qiao, Y.Q.Wang, Z.R.Shi, M.Gu, Nano Lett 2012, 12 (5), 2187-2192.
7. R. J. Liu, S. W. Li, X. L. Yu, G. J. Zhang, Y. Ma, J. N. Yao, B. Keita, L. Nadjo, Cryst. Growth. Des. 2011, 11, 3424-3431.
8. Q.L.Huang, X.S.Zhu, Materials Chemistry and Physics. 2013, 138, 689-694.
9. Y.L.Wang, P.H.C.Camargo, S.E.Skrabalak, H.C.Gu, Y.N.Xia, Langmuir 24 (2008) 12042-12046.
10. W. Ren, S. Guo, S. Dong, E. Wang, J. Phys. Chem. C 115 (2011) 10315
11. N. A. Hatab, C. H. Hsueh, A. L. Gaddis, S. T. Retterer, J. H. Li, G. Eres, Z. Y. Zhang and B. H. Gu, Nano Lett, 2010, 10, 4952-4955.
12. Y. Q. Wang, T. Gao, K. Wang, X. P. Wu, X. J. Shi, Y. B. Liu, S. Y. Lou and S. M. Zhou, Nanoscale, 2012, 4, 7121-7126.
13. C. H. Zhu, G. W. Meng, Q. Huang, Z. Zhang, Q. L. Xu, G. Q. Liu, Z. L. Huang, and Z. Q. Chu, Chem. Commun, 2011, 47, 2709-2711.
14. S. K. Yang, W. P. Cai, L. C. Kong, Y. Lei, Adv. Func. Mater, 2010, 20, 2527–2533.
15. J. Zeng, Y. Q. Zheng, M. Rycenga, J. Tao, Z.Y. Li, Q. Zhang, Y. M. Zhu, Y. N. Xia. J.Am. Chem. Soc. 2010, 132, 8552-8553.
16. Y. G. Sun, B. Gates, B. Mayer, Y. N. Xia. Nano Lett. 2002, 2 (2), 165-169
17. B. H. Lee, M. S. Hsu, Y. C. Hsu, C. W. Lo, C. L. Huang. J. Phys. Chem. C, 2010, 114, 6222.
18. M. V. Mandke, S. H. Han, and H. M. Pathan, CrystEngComm, 2012, 14, 86-89.
19. F. Huang, H. Z. Zhang and J. F. Banfield, Nano Lett, 2003, 3, 373.
20. K. J. Vetter, Electrochemical Kinetics-Theoretical and Experimental Aspects, Acadamic Press, New York, 1967.
21. L. T. Qu, L. M. Dai, J. Phys. Chem. B, 2005, 109, 13985-13990.
22. G. X. Zhang, S. H. Sun, M. N. Banis, R. Y. Li, M. Cai and X. L. Sun, Cryst. Growth. Des. 2011, 11, 2493-2499.
23. A. V. Avizienis, C. M. Omos, H. O. Sillin, M. Aono, J. K. Gimzewski, A. Z. Stieg, Cryst. Growth. Des. 2013, 13, 465-469.
24. W. C. Ye, D. A. Wang, H. Zhang, F. Zhou, W. M. Liu, Electrochimica Acta. 2010, 55, 2004-2009.

Ag nanosheet-assembled microsphere @ Ag dendrites core-shell hierarchical architectures with excellent SERS performance are successfully synthesized.